



UNIVERSITY OF COLORADO BOULDER

ASEN 2002: INTRODUCTION TO THERMODYNAMICS/AERODYNAMICS

Calibration of the ITLL Low-Speed Wind Tunnel

Authors:

A. ALAMERI, F. GREER, C. MAITLAND, J. SOLTYS
(GROUP 2)

November 14, 2018

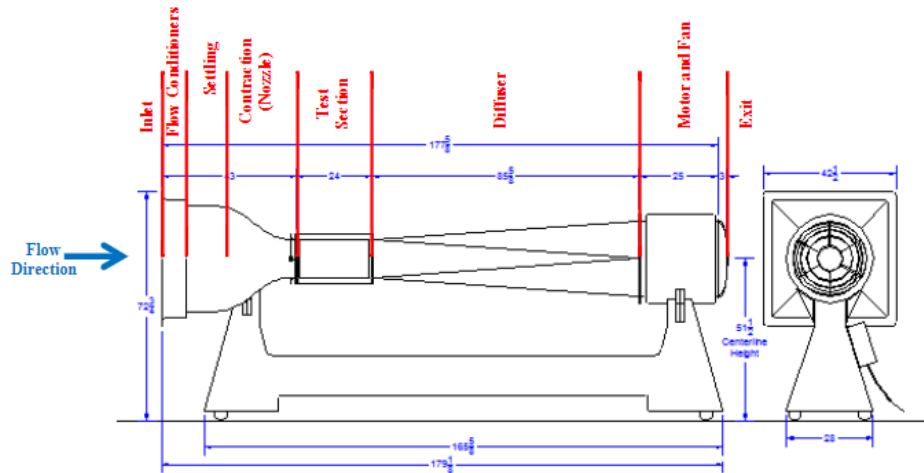


Figure 1: figure 0 : ITLL Low speed wind tunnel

1 Variable Nomenclature

ρ = Density of fluid ($\frac{kg}{m^3}$)

\vec{V} = Velocity of fluid ($\frac{m}{s}$)

P = Pressure (kPa)

R = Gas constant for air = 0.2870 ($\frac{J}{kg*K}$)

T = Temperature (K)

A = Cross sectional area of fluid flow (m^2)

δ = Boundary layer Thickness (m)

Re = Reynolds number

x = Horizontal location within test section

RSS = Sum of the Squares of the Errors

Note: The variables above are listed generally. Values are specified using subscripts.

Abstract

This paper outlines the operation of the ITLL Low-Speed Wind Tunnel and the basic concepts and definitions associated flow measurements and wind tunnel testing. Flow velocity can be quantified using basic aerodynamic principles and measurement devices and sensors, such as pressure measurement devices, and temperature sensors. Ambient temperature was measured with an LM35 Precision Centigrade Temperature Sensor. Two experiments were conducted, the first tends to focus on the relationship between voltage of inputs to operate the fan at the ITLL and the second to examine the effect of the boundary layer on the flow. For the first experiment, two measurement configurations were used to quantify the air speed included a Pitot-Static Probe, and a Venturi Tube setup. Each of the two setups used either a U-Tube water Manometer as a pressure differential device or Airspeed Pressure Transducer. Our group measured the pressure difference using the Airspeed Pressure Transducer with the Pitot-Static tube configuration and U-Tube water Manometer with the Venturi tube configuration. Our group measured data at the voltages: 1V, 3V, 5V, 7V, and 9V. Electronic measurements collected 500 data points at each voltage, and U-Tube measurements were visually measured by group members. Air speed was calculated relating ambient temperature and measured pressure differentials using the Continuity equation and Bernoulli's equation. These calculations yielded: very similar air velocity values at each voltage with minor differences (table 1). The general trend was an increase of velocity with respect to voltage (figure 2). The second experiment, the boundary layer, measured the free-stream velocity at a constant voltage (5V) and attempted to understand how the free-stream velocity change going further along the length of the wind tunnel. While an increase in the free-stream velocity was expected, the measured increase was not able to be quantified due to errors in data gathering, which discussed heavily in section 5.

2 Introduction

This lab explores the basic foundations of wind tunnel operations to serve as an introduction to the tool before moving to more complicated applications. As such, discussion includes basic concepts of flow measurement and the application of error analysis techniques to the observed measurements. Conservation of mass and Bernoulli's equations (assuming that our flow is slow enough to be treated as incompressible flow without a noticeable amount of error) are used to estimate the airspeed in the test section at different fan voltages. Pressure difference measurements were taken using two different setups: a Pitot-Static Probe, which used a pressure transducer to measure a pressure differential, and a Venturi Tube setup, which used a U-Tube Manometer as a measurement device. In addition, the formation of viscous boundary layers inside the wind tunnel and its effects on the center-line flow are also modeled. Comprehension of the lab procedure, measurement process, analysis, and the findings detailed later in this report will contribute to successful use of the wind tunnel further on in the aerospace program.

3 Experimental Setup and Measurement Techniques

Since there is no way to measure airspeed directly, it is quantified by relating other properties that can be measured directly, specifically the temperature and pressure differential of the flow. Data collection was split between Experiment 1 and Experiment 2. Experiment 1 measured pressure differentials at a static point while (discretely) increasing input voltages. Multiple configurations were used to gather data, which are detailed in the following sections. The input voltage was then related to air speed after calculating the flow velocity at each respective voltage. Experiment 2 was to measure the affect of the boundary layer on the flow velocity. Input voltage was held constant and pressure measurements were taken at different heights (Y values) in the test section. In order to make these calculations we assume the the flow is 1) steady, 2) uniform, 3) inviscid, and 4) incompressible.

Due to the large amount of measurements needed to accurately analyze the test section, data gathering was partitioned between lab groups. We (Group 2) partnered with Group 1 to take measurements. In Experiment 1, the Pitot-Static Probe setup used a pressure transducer to measure the pressure differential. The Venturi Tube setup used a U-Tube Manometer as a measurement device. Measurements taken at voltages: 1V, 3V, 5V, 7V, and 9V. Electronic measurements collected 500 data points at each voltage, and U-Tube measurements were visually measured and recorded by group members.

3.1 Ambient Temperature and Pressure

Ambient temperature, T_{atm} , and Ambient pressure P_{atm} were measured with an LM35 Precision Centigrade Temperature Sensor, and pressure transducers, which is assumed to be the static properties and the total form the reservoir, i.e. the room. Temperature measurements and pressure were recorded at each data point in order to relate them to the density of the fluid, via the ideal gas law and the derived velocity formulas from Bernoulli's (Section 7.2, (7,8,9)).

3.2 Pressure difference

Pressure difference was experimentally measured using two different configurations, each with their own unique measurement device. These devices included a U-Tube Manometer and a piezoresistive transducer (pressure transducer). The U-tube water manometer provided a visual representation of pressure differential and the Honeywell SCX01DN differential pressure sensors provided a numerical one.

3.2.1 Pitot-Static Probe

The first configuration measured the differential with a Pitot-Static Probe, that used the transducer to measure the pressure difference, ΔP , using static pressure and total pressure. The probe was mounted in the test section, allowing us to find these pressure values at a single point in the flow. It is assumed that the initial velocity of the air is 0. Since the air in the lab is relatively stagnant compared to the flow, the lab acts as a reservoir and this assumption is justified. With all of our assumptions, we can now rearrange Bernoulli's equation to solve for the free stream velocity. The probe provides an accurate measurement of flow velocity, but introduces a wake created by the probe body. Consequently, this could affect test model results when actually using the test section.

3.2.2 Venturi Tube

The second configuration compares the average static pressures at the settling chamber and the test section. A U-Tube manometer was hooked up to the different sections of the wind tunnel. The difference in their pressures compared to the cross-sectional areas of the wind tunnel at that point drives a pressure differential within the tube, which then causes a displacement in the static head of the fluid inside. The fluid inside the Dwyer Flex-Tube U-Tube manometer we used has a known specific gravity of 0.826. Since we are comparing two cross sectional areas that have some velocity, we cannot assume that one of the velocities is zero and the law of conservation of mass must be utilized. This law, along with Bernoulli's equation, is known as the Venturi Tube equation (Section 7.2,(6,8,9)), and is listed below in the airspeed calculation section. This configuration eliminates the need for a probe within the flow, but introduces other errors, such as a lack of precision in manual U-Tube readings.

3.3 Other Groups

The details above list the configurations used in gathering our own group's data. Each other group followed other procedures and configurations in order to cover a wide array of data, allowing for a thorough analysis. For Experiment

1, this includes switching measurement devices for each configuration and measuring at different voltage sets, or some combination of the two. Experiment 2 had variance in ports (X locations) and heights (Y locations) within the test section where ΔP was measured.

4 Airspeed Calculation and Airspeed Model

To compute the airspeed inside the test section, it was assumed that the air inside the wind tunnel acts as an ideal gas and it is slow enough to be treated as incompressible flow. This allows the application of Bernoulli's Equation solved for airspeed inside the test section. MatLab scripts and functions (see Appendix, Matlab Codes) were written to loop through the data collected by the airspeed pressure transducer and water manometer setups and produce a mean value for temperature, atmospheric pressure, and the pressure differential recorded at each voltage value. The mean values of the Pitot-Static setup were then substituted into Equation 8 to produce an airspeed velocity at each voltage for both measurement setups, while the mean values of the manometer setup were substituted into Equation 9 to obtain airspeed velocity (Figure 2).

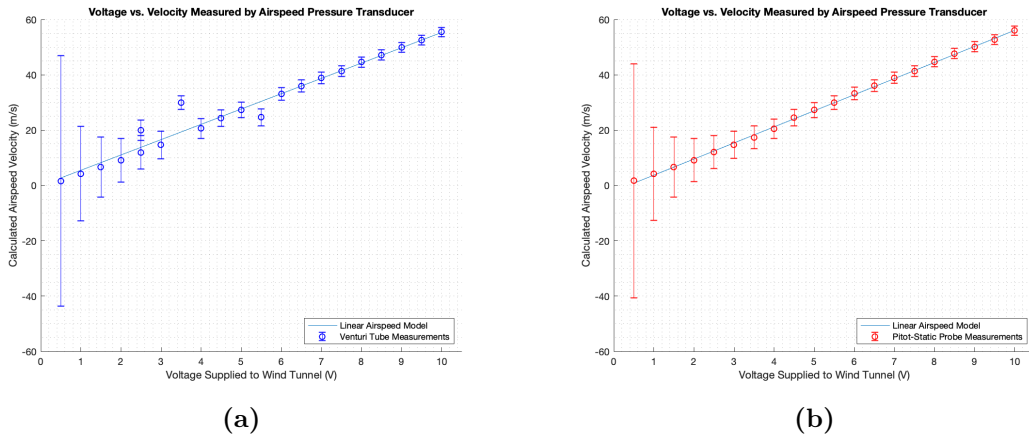


Figure 2: Calculated velocity and associated error for a range of 0.5-10 volts using
(a) Venturi Tube, **(b)** Pitot-Static Probe

The air speeds calculated by Bernoulli's equation using the data collected by both the manometer and the pitot-static probe are both extremely similar, and can be seen in Figure 2 above. Due to the manometer data being collected via a visual reference, instead of being computed outright with sensor-measured data as it is in the pressure transducer, it is understandable that this method of collection can cause the manometer-computed airspeed to deviate from that of the pressure transducer values. It is also worth noting from figure 2 that as airspeed increases, the error decreases. This general trend tells us that the wind tunnel at the ITLL gives more accurate results when run at higher voltage and resultant velocities. As the area ratio between the wind tunnel settling chamber and test section increases, the velocity of air through the test section in subsonic flow conditions will increase. As the ITLL Low-Speed Wind Tunnel is subsonic, increasing this area ratio will thus allow for scale-model designs and wing sections to be tested in a larger range of conditions.

Through analysis of the recorded data and calculation of airspeed velocity inside the test section at different voltages, a linear relationship between supplied voltage and resultant velocity was discovered (figure 3). Fitting a line to the data showed that this relationship could be approximated by the equation

$$\vec{V} = 5.67V - 1.01 \text{ m/s},$$

where \vec{V} is the airspeed velocity and V is the supplied voltage. Thus, this equation can be used to solve for the required input voltage to create any desired airspeed in the wind tunnel test section. It is worth noting that both configurations exhibit some what similar trend in terms of error analysis, and as explained above and in the error analysis section, the error decreases as voltage increases. However, it is worth noting also that the data of the Venturi tube configuration is closer to the best fit, and that might indicate that the Venturi tube set-up might lead to better results.

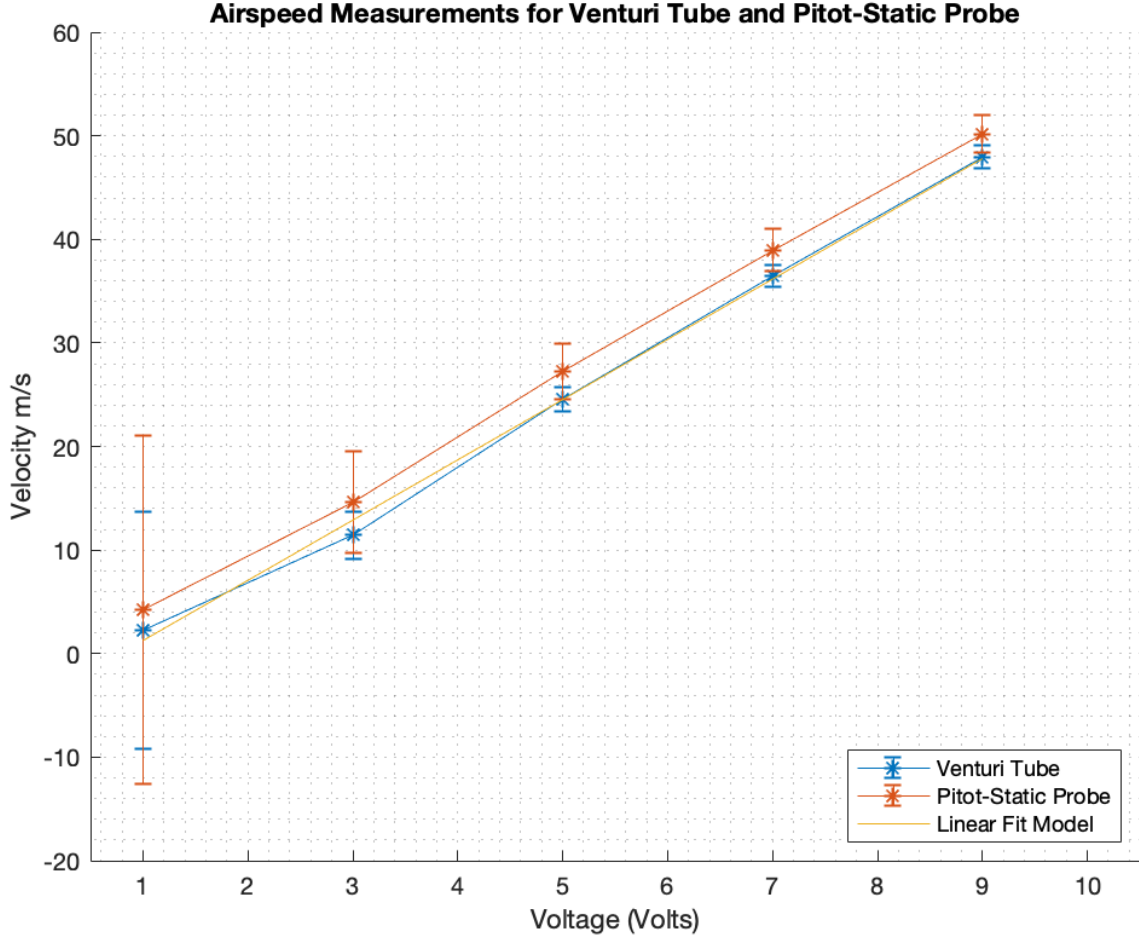


Figure 3: Resultant velocity vs applied voltage

Voltage (V)	P. S. Velocity (m/s)	P. S. Error (m/s)	Vent. Velocity (m/s)	Vent. Error (m/s)
1	4.2742	16.8084	2.2861	11.430
3	14.6651	4.9080	11.4300	2.2983
5	27.2817	2.6935	24.5152	1.1812
7	38.9731	2.0131	36.4337	1.0424
9	50.1898	1.7704	47.9521	1.1349

Table 1: Calculated velocities at various voltage settings, with error

5 Airspeed Measurement Uncertainty

As with any experiment, error is encountered in the collection of data. We used both the general method and step-by-step method [1] to develop equations for the uncertainties in our airspeed measurements to have an additional check. These formulas assume that the R value for air and the area ratio $\frac{A_2}{A_1}$ have no associated uncertainty. Equation 10 describes the formulation for this equation using the general method. The partial derivatives that are put in to this equation are shown in equations 11 through 13. The final expressions for the uncertainties in the velocity measurements that we developed are shown by equations 1 for the uncertainty in the velocity calculated by the Pitot-Static Probe and 2 for the uncertainty in the Venturi Tube.

$$\sigma_{\bar{v}_\infty} = \frac{1}{2} \sqrt{\frac{2\Delta P R T_{atm}}{P_{atm}}} \sqrt{\left(\frac{\sigma_{\Delta P}}{\Delta P}\right)^2 + \left(\frac{\sigma_{T_{atm}}}{T_{atm}}\right)^2 + \left(\frac{\sigma_{P_{atm}}}{P_{atm}}\right)^2} \quad (1)$$

$$\sigma_{\bar{V}_\infty} = \frac{1}{2} \sqrt{\frac{2\Delta P R T_{atm}}{P_{atm} \left(1 - \left(\frac{A_2}{A_1}\right)^2\right)}} \sqrt{\left(\frac{\sigma_{\Delta P}}{\Delta P}\right)^2 + \left(\frac{\sigma_{T_{atm}}}{T_{atm}}\right)^2 + \left(\frac{\sigma_{P_{atm}}}{P_{atm}}\right)^2} \quad (2)$$

Both the manometer and pitot-static probe measurements have similar error in each individual measurement, shown in the graphs below. Further, both measurement systems have a similar trend in the precision of their data as voltage supplied to the wind tunnel increases. However, the manometer measurements included values at 2.5, 3.5, and 5.5 volts that do not fit the general trend of the line of best fit calculated for our airspeed relation. These half-volt values were not collected by this lab group and thus the reason for this discrepancy cannot be confidently determined.

Collected data suggests that the U-Tube manometer is inherently less accurate in the computing of airspeed through the test section. This is due to both the limited precision of the instrument itself (gradation on the manometer is given in 0.1 inch sections) and also the inaccuracy introduced into the data when it is collected by the human eye. This includes error from reading the scale at an angle, refraction from reading the height of the liquid inside through the glass surround, and the possibility of reading the scale at the height of the meniscus formed on the sides of the glass surround instead of the correct value at the bottom of the meniscus.

The largest sources of uncertainty in the data collected come from the error in the observed pressure and differential pressure values. The amount of error in these calculations is dependent on the manufacturer-quoted accuracy of the sensors and instruments used in the lab, with the Freescale MPX4250A Absolute Pressure Sensor having an error of ± 3450 Pa for observed pressure and ± 68.95 Pa for differential pressure. Outside of purchasing data collection instruments with higher precision, these values cannot be improved, and instead must be taken into account when calculating test section velocity and the error associated with said calculations and then further described in the report. As the uncertainty in the absolute pressure sensor is quite large compared to the other uncertainties in the experiment, it makes sense that the biggest improvement in the uncertainty in measured airspeed would come from improving the accuracy of the Free-scale Absolute Pressure Sensor. Due to this, the general trend is noticed in both Table 1, figure 2, and figure 3, as the voltage increases, the uncertainty decreases, and that is to say, the wind tunnel operates better and more accurately on high voltages rather than lower ones.

6 Boundary Layer Influence

Since the wind tunnel is not a perfect system, an accurate analysis of the flow velocity must account for drag close to the walls of the test section. This friction between the surface of the test section and the air flowing over it forms a boundary layer, or a layer of fluid with lowered velocity. The boundary layer thickness is defined as the location at which airspeed reaches 0.95 of the free-stream velocity in the test area. There was more than one way to about this, and the chosen way after studying the general trend of the boundary layer behavior, is to fit a curve to the data using MATLAB curve fitting tool. Using the best fit function (figure 4), which was function of velocity that returns thickness, the thickness was determined as the thickness when the velocity is 0.95 of the free-stream velocity. The function that was thought to be best for the fit is a rational function that has a 4th degree numerator and denominator. The error associated with this thickness was taken to be the error of the fitted data, using the RSS values resulted from the fit.

6.1 Boundary Layer Height Prediction

The theoretical height of the boundary layer was predicted using equations stated in Chapter 4 of Anderson's *Introduction to Flight*.

$$\delta_T = \frac{0.37x}{(Re_x)^{0.2}} \quad (3)$$

$$\delta_L = \frac{5.2x}{\sqrt{Re_x}} \quad (4)$$

Where the first equation models the turbulent boundary layer height and the second predicts the laminar boundary layer height. They are both functions of the x position in the testing section and the local Reynolds number at that x position. Our predicted turbulent height at port 1 was 1.7mm and the laminar height was 0.0668mm.

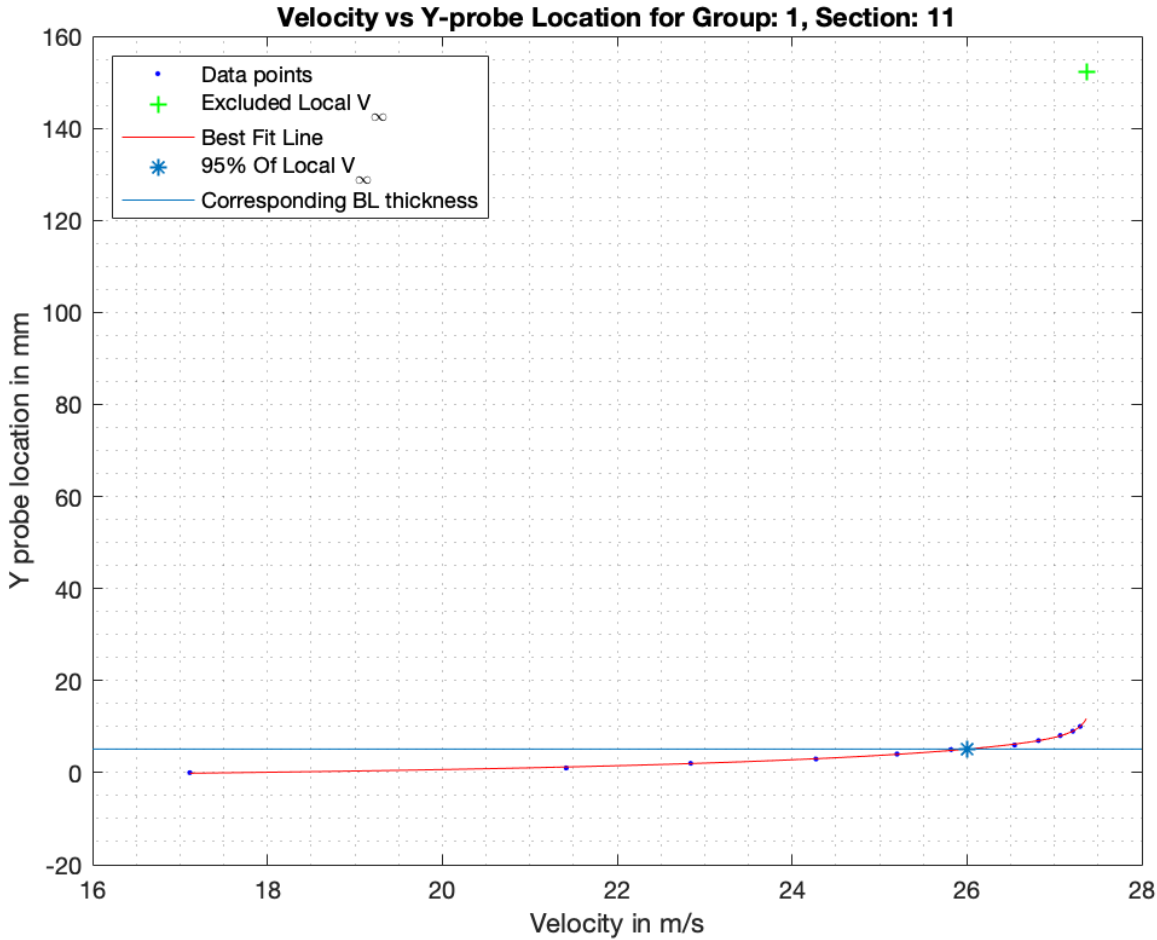


Figure 4: Determination of boundary layer thickness

6.2 Boundary Layer Height Measurements

To measure the actual height of the boundary layer we calculated the velocity at each height for each probe. Each group was assigned a specific port, which corresponded to some X location within the test chamber. Each group was also tasked with taking measurements at increasing Y values (Y probe location, or heights), including the center-line. The top of the boundary layer is considered to be where this calculated height was 95% of the free stream velocity. This is summarized by equation 5 listed below.

$$\delta = y @ \vec{V} = 0.95 \vec{V} \quad (5)$$

The actual boundary layer height at port 1 was calculated to be 5.11mm. When compared to our predicted boundary layer height, we see a difference of 200%. This difference can be attributed to the fact that there is a surface that interacts with the flow in the settling chamber. This effectively increases our x value, since we define the zero to be the beginning of the test chamber, at the actual leading edge where the flow meets the settling chamber surface. The graph below plots the boundary layer data.

From figure 5, it is most likely that the boundary layer at port 1 was turbulent, since the data matches closer to the turbulent shape (plotted in green). Other group's data is also plotted on this graph. As we move farther down the test section, the boundary layer increases. This increase takes the shape of a \sqrt{x} function (or generally a root function). This trend matches the equations above for the height predictions, since the Reynolds number is taken to the power of less than one. The affect on the free stream velocity is discussed next.

It is important to note that we had to exclude some of the groups data that had some issues with their files. Table 2 shows the groups that were excluded and the reason. Although excluding some groups for having more or less data is generally not a good reason, we decided to do that because we wanted to make the functions and routines as

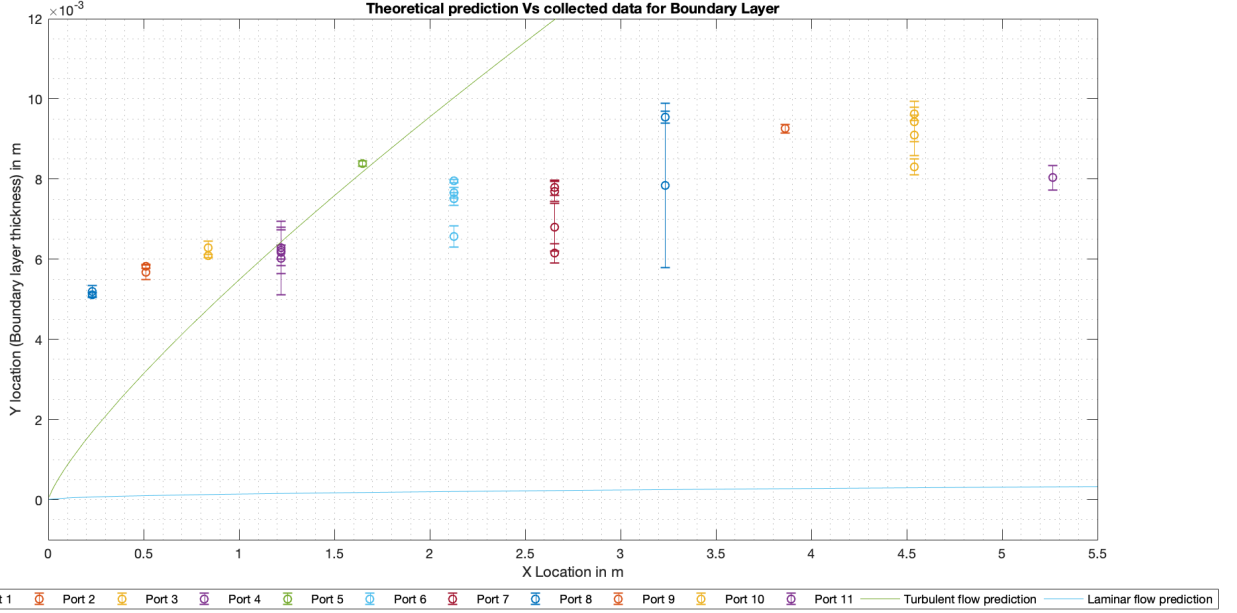


Figure 5: Boundary Layer data: Note that both scales in X and Y are multiplied by $e-3$. MATLAB only shows one in top of the figure

Group	Section	Reason of exclusion
7	12	Skipped taking data at a y-probe location of 5.5 mm
13	12	Did not change the y-probe location at all. Started and finished at 0 mm.
11	13	Did not take measurements at the free-stream section.
5	14	Around 2000 data point per y-probe location, way more than all the generic files that are used.
7	14	Skipped taking data at a y-probe location of 0 mm.

Table 2: Excluded groups and reason of exclusion

autonomous as possible. There was two ways to do that, either by depending on the same frequency of data collecting, which most groups used, or using an adaptable method to detect the change within the location of the y-probe. The problem with the second approach that it can deviate easily if there is any error in the instrument, and the mistake might not be noticed, and thus the first method was chosen, and hence the groups that did not follow the same exact procedure were excluded. Fortunately, the number of excluded groups was not that massive to effect the results of the experiment.

Figure 6 shows the free stream velocity at each port location. Based on rearrangements in Bernoulli's equations and steady flow conditions, the free-stream velocity was predicted to be 27.325 m/s , and the calculated free-stream velocity was 27.365 m/s , which matched our prediction very well with a relative error of 0.14% .

The free stream velocity was expected to increase by the area ratio defined by the test section entrance area and the boundary layer dimensions. This was not the case, as clearly reflected by the graph above. This error is most likely due to different groups not zeroing at the same exact Y location when measuring the boundary layer. Some groups may have crashed the probe, causing a bias in one direction, and other groups may have zeroed without touching off, giving another bias in the opposite direction.

Unfortunately, no measurable conclusion on the center-line velocity can be made. As discussed, those deviation can be either to a mistakes in calibration or in taking the data.

7 Conclusion

Through the relation of experimentally measured quantities across a range of voltage settings and probe locations from different lab groups, the airspeed in the test section was found to be linearly related to the voltage supplied. Specifically, this relation can be quantified by the equation $\vec{V} = 5.67V - 1.01 \text{ m/s}$, and thus allows for the determination of the exact voltage needed to create a certain test-section velocity inside the wind tunnel. Computing airspeed from

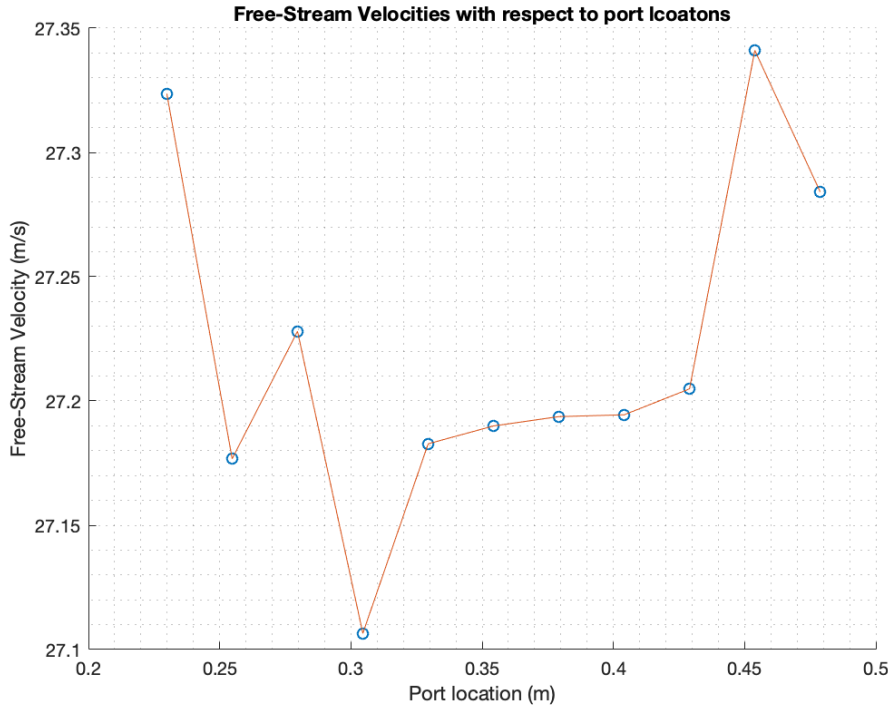


Figure 6: This graph shows a seemingly random affect on the free stream velocity from the boundary layer

pressure data collected by the pressure transducer setup was preferred to the manometer setup, as it removes the possibility of human error in the calculations and is then only subject to a predefined, static level of uncertainty when used for calculation. In addition, it seemed like that the Venturi Tube configuration in general is a better configuration, since it was closer to the linear fit.

When it come to the Boundary Layer effect, it is hard to make a decisive judgment due to the errors in the data, however it seems that the boundary layer does affect the free stream velocity of the wind tunnel, due to the low thickness in general.

With that being said, one common trend that was noticed is that the error gets smaller and smaller as the voltage the wind tunnel opreates on increases.

8 Appendix

8.1 Final Equation List

$$P_1 + \frac{1}{2}\rho\vec{V}_1^2 = P_2 + \frac{1}{2}\rho\vec{V}_2^2 \quad (6)$$

$$\rho = \frac{P}{RT} \quad (7)$$

$$\vec{V}_\infty = \sqrt{2\Delta P \left(\frac{RT_{atm}}{P_{atm}} \right)} \quad (8)$$

$$\vec{V}_\infty = \sqrt{\frac{2(P_{s,1} - P_{s,2})}{\rho(1 - (\frac{A_2}{A_1})^2)}} = \sqrt{\frac{2\Delta P R T_{atm}}{P_{atm}[1 - (\frac{A_2}{A_1})^2]}} \quad (9)$$

$$\delta\vec{V} = \sqrt{\left(\frac{\partial\vec{V}}{\partial\Delta P}\delta\Delta P\right)^2 + \left(\frac{\partial\vec{V}}{\partial P_{atm}}\delta P_{atm}\right)^2 + \left(\frac{\partial\vec{V}}{\partial T_{atm}}\delta T_{atm}\right)^2} \quad (10)$$

$$\frac{\partial\vec{V}}{\partial\Delta P} = \frac{RT_{atm}}{2[1 - (\frac{A_2}{A_1})^2]\sqrt{\frac{\Delta P R T_{atm}}{P_{atm}[1 - (\frac{A_2}{A_1})^2]}}}(P_{atm}) \quad (11)$$

$$\frac{\partial\vec{V}}{\partial P_{atm}} = \frac{-\Delta P R T_{atm}}{2[1 - (\frac{A_2}{A_1})^2]\sqrt{\frac{\Delta P R T_{atm}}{P_{atm}[1 - (\frac{A_2}{A_1})^2]}}}(P_{atm})^2 \quad (12)$$

$$\frac{\partial\vec{V}}{\partial T_{atm}} = \frac{\Delta P R}{2[1 - (\frac{A_2}{A_1})^2]\sqrt{\frac{\Delta P P_{atm} R_{atm}}{P_{atm}[1 - (\frac{A_2}{A_1})^2]}}} \quad (13)$$

$$\delta_T = \frac{0.37x}{(Re_x)^{0.2}} \quad (14)$$

$$\delta_L = \frac{5.2x}{\sqrt{Re_x}} \quad (15)$$

8.2 References

- [1] Turner, J. R., "General Formula for Error Propagation," An Introduction to Error Analysis: The Study of Uncertainties in Physical Measurements, 2nd ed., University Science Books, Sausalito, CA, 1996, pp. 73–78.

8.3 Manometer Images

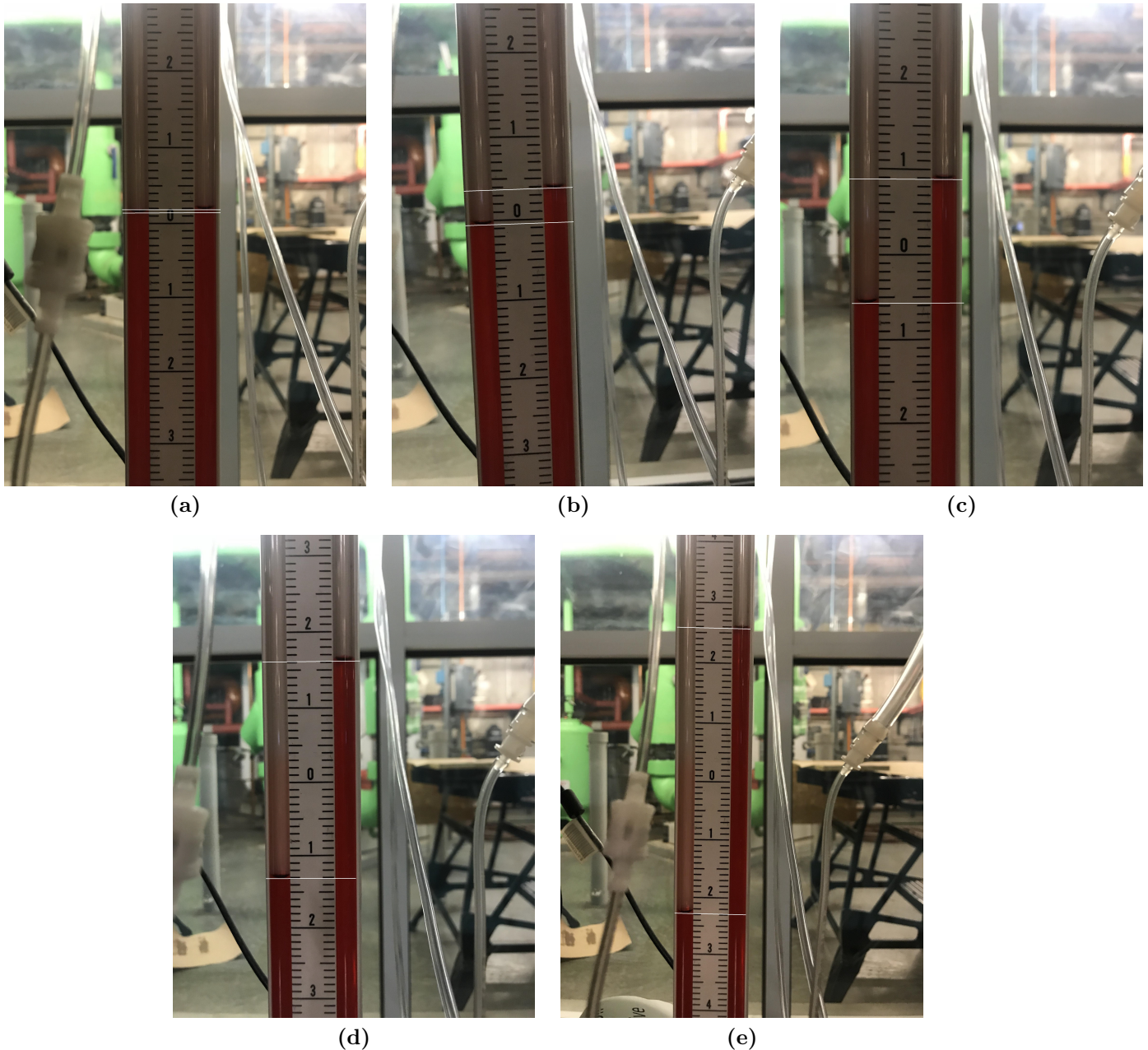


Figure 7: Water Manometer pressure differential readings at several voltages (a) 1V (b) 3V (c) 5V (d) 7V (e) 9V